



Minerva Access is the Institutional Repository of The University of Melbourne

Author/s:

Sturges, BK;Kapatkin, AS;Garcia, TC;Anwer, C;Fukuda, S;Hitchens, PL;Wisner, T;Hayashi, K;Stover, SM

Title:

Biomechanical Comparison of Locking Compression Plate versus Positive Profile Pins and Polymethylmethacrylate for Stabilization of the Canine Lumbar Vertebrae

Date:

2016-04-01

Citation:

Sturges, B. K., Kapatkin, A. S., Garcia, T. C., Anwer, C., Fukuda, S., Hitchens, P. L., Wisner, T., Hayashi, K. & Stover, S. M. (2016). Biomechanical Comparison of Locking Compression Plate versus Positive Profile Pins and Polymethylmethacrylate for Stabilization of the Canine Lumbar Vertebrae. *Veterinary Surgery*, 45 (3), pp.309-318. <https://doi.org/10.1111/vsu.12459>.

Persistent Link:

<https://hdl.handle.net/11343/291090>

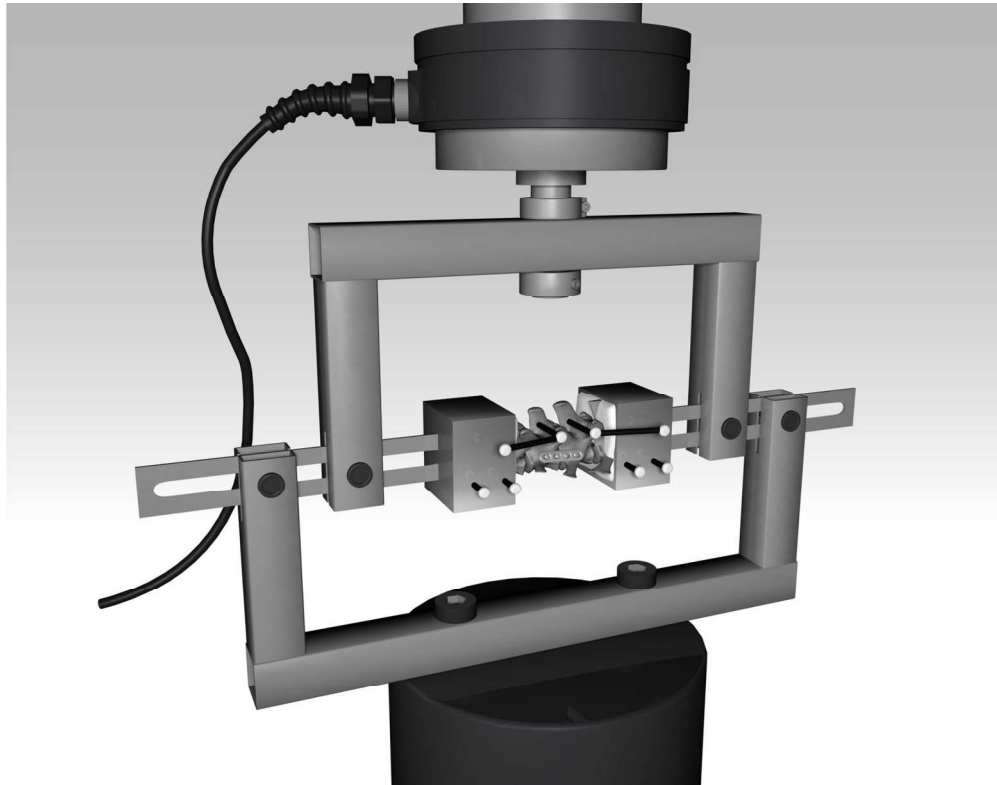


Figure 1  
177x138mm (300 x 300 DPI)

Accep

This is the author manuscript accepted for publication and has undergone full peer review but has not been through the copyediting, typesetting, pagination and proofreading process, which may lead to differences between this version and the [Version record](#). Please cite this article as [doi:10.1111/vsu.12459](https://doi.org/10.1111/vsu.12459).

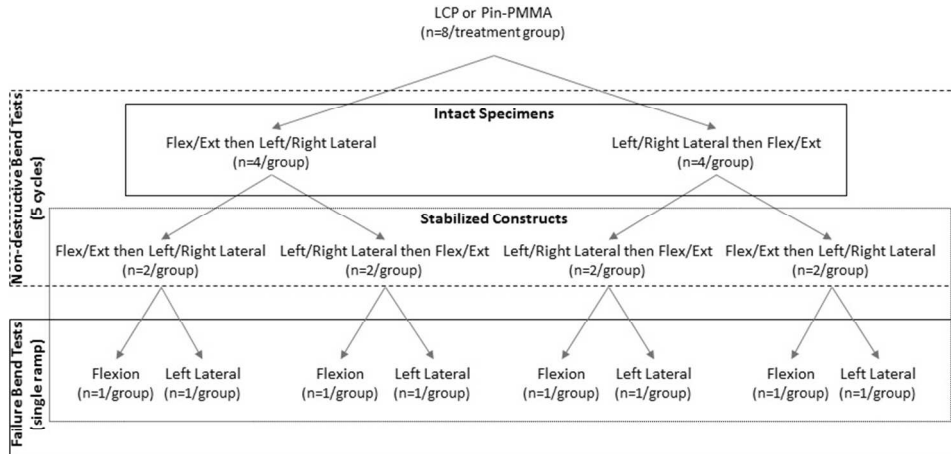


Figure 2  
254x190mm (96 x 96 DPI)

Accep1

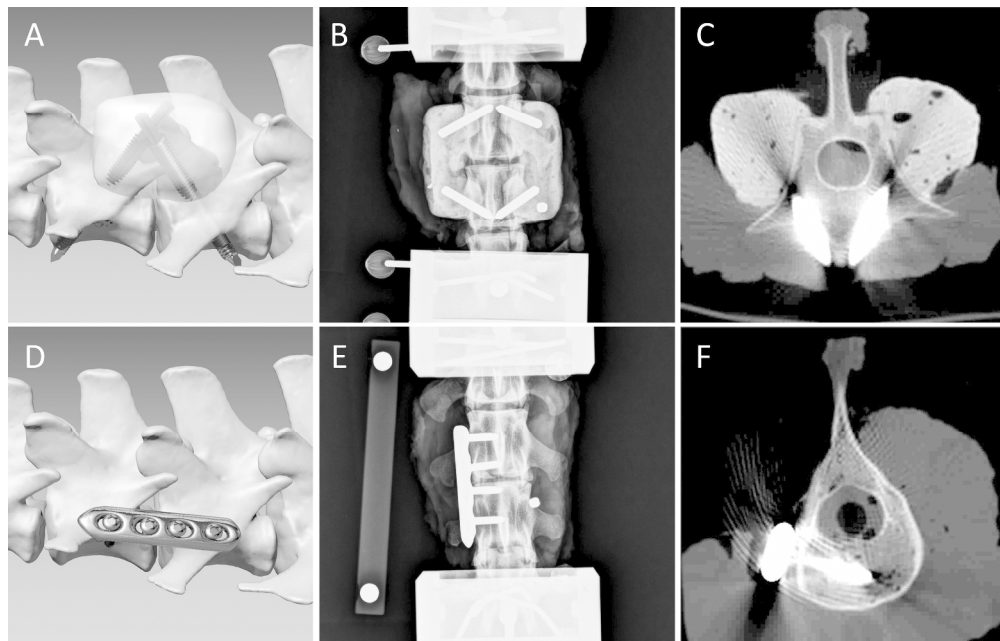


Figure 3  
315x200mm (300 x 300 DPI)

Accepte

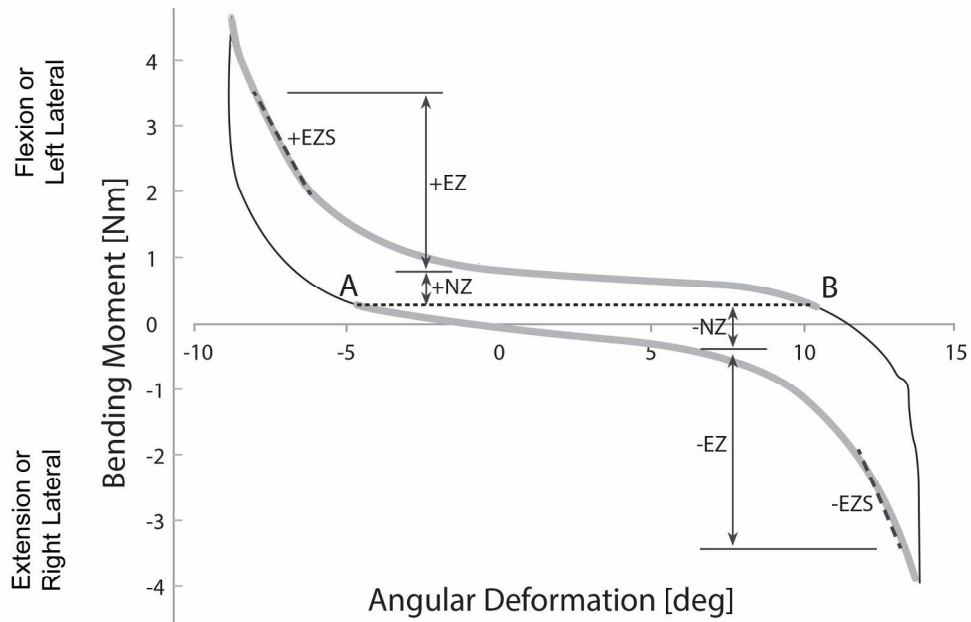


Figure 4  
195x131mm (300 x 300 DPI)

Accept

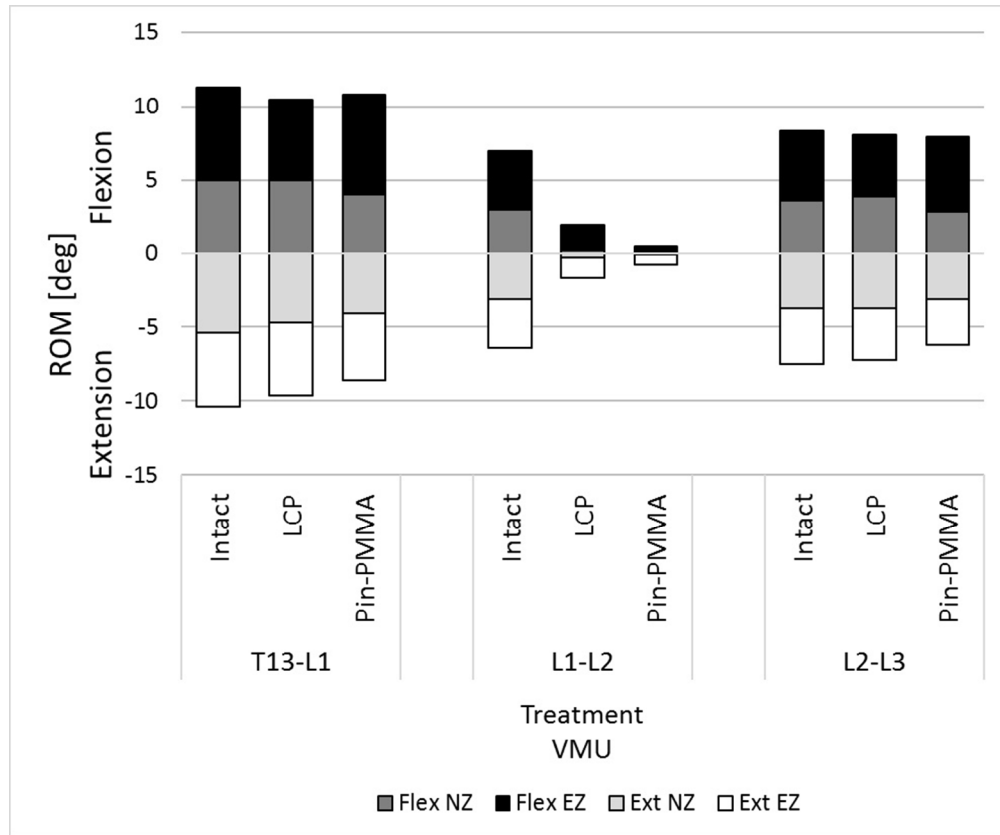


Figure 5a  
167x139mm (150 x 150 DPI)

Accepted

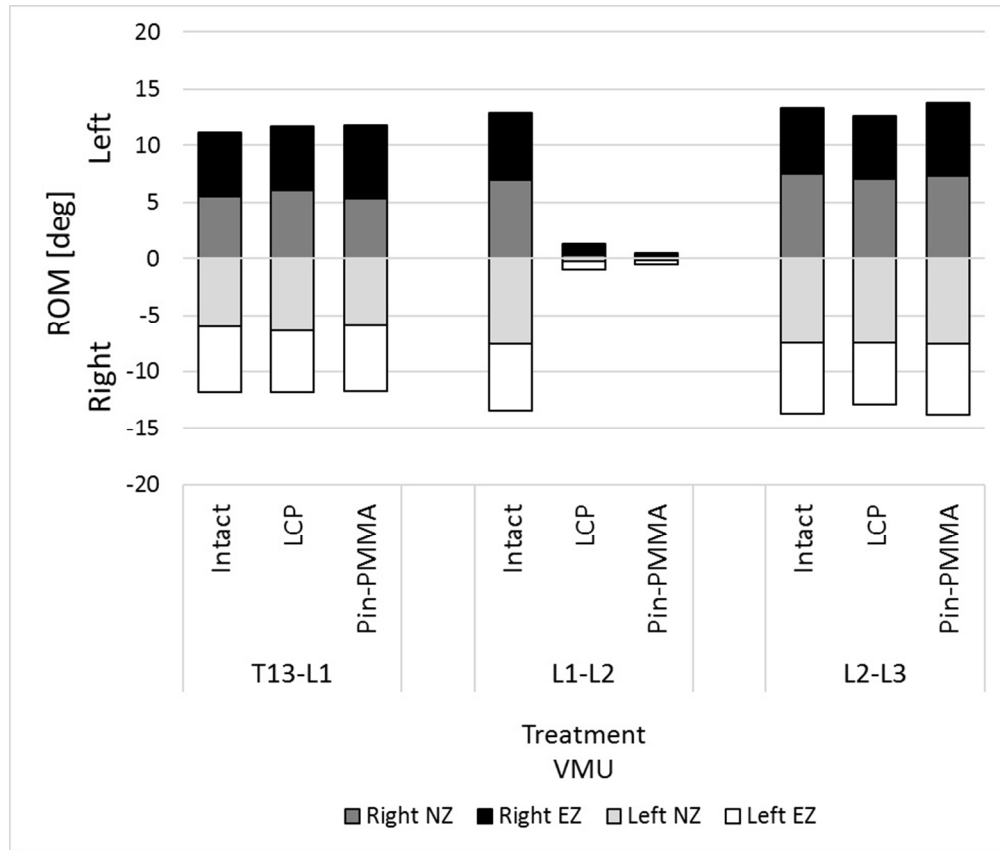


Figure 5b  
165x140mm (150 x 150 DPI)

AcceJ

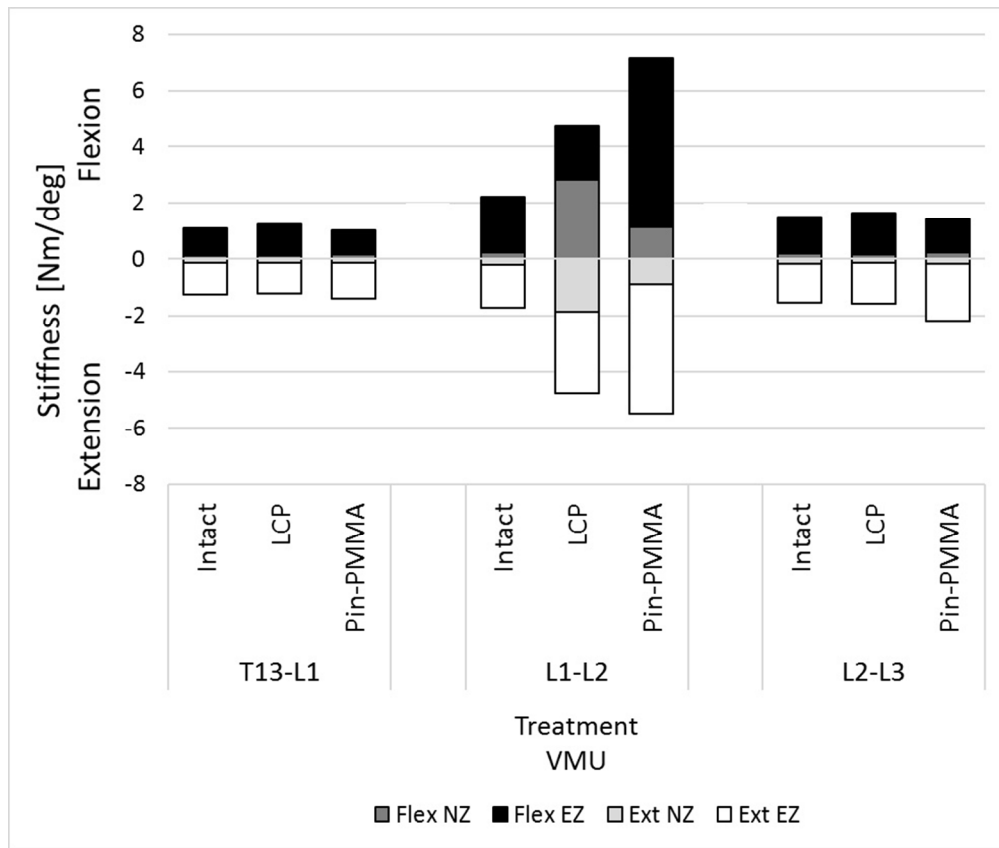


Figure 6a  
166x140mm (150 x 150 DPI)

AcceJ

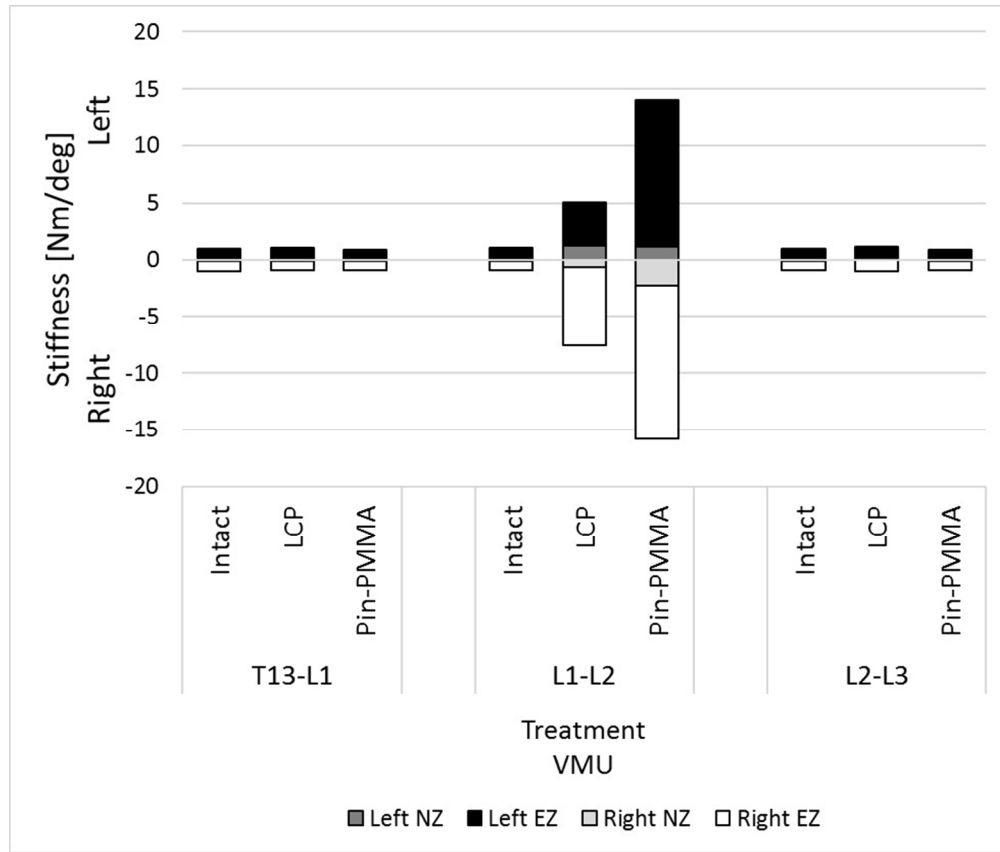


Figure 6b  
166x141mm (150 x 150 DPI)

AcceJ

Biomechanical Comparison of Locking Compression Plate versus Positive Profile  
Pins and Polymethylmethacrylate for Stabilization of the Canine Lumbar  
Vertebrae

Beverly K. Sturges<sup>1</sup>, Amy S. Kapatkin<sup>1</sup>, Tanya C. Garcia<sup>2</sup>, Cona Anwer<sup>3</sup>,  
Shimpei Fukuda<sup>2</sup>, Peta L. Hitchens<sup>2</sup>, Tristan Wisner<sup>2</sup>, Kei Hayashi<sup>1</sup> and Susan  
M. Stover<sup>2</sup>

<sup>1</sup>Department of Surgical and Radiological Sciences, <sup>2</sup>JD Wheat Veterinary  
Orthopedic Research Laboratory, <sup>3</sup>William R. Pritchard Veterinary Teaching  
Hospital, School of Veterinary Medicine, University of California-Davis, CA

Submitted February 2015

Accepted October 2015

**Corresponding Author**

Beverly K. Sturges,  
Department of Surgical & Radiological Sciences  
1 Shields Avenue  
Davis, CA 95616  
bksturges@ucdavis.edu

Presented, in part, at the One AO Conference, Las Vegas, NV, February 2015

Running header: Locking Compression Plate vs Positive Profile Pins/PMMA for

Lumbar Vertebrae

Accepted Article

**Objective:** To compare the stiffness, angular deformation and mode of failure of lumbar vertebral column constructs stabilized with bilateral pins and polymethylmethacrylate (Pin-PMMA) or with a unilateral (left) locking compression plate with monocortical screws (LCP).

**Study Design:** Ex vivo biomechanical, non-randomized

**Samples:** Cadaveric canine thoracolumbar specimens (n=16)

**Methods:** Thoracolumbar (T13-L3) vertebral specimens had the L1-L2 vertebral motion unit stabilized with either Pin-PMMA or LCP. Stiffness in flexion, extension, and right and left lateral bending after nondestructive testing were compared between intact (pre-treated) specimens and Pin-PMMA, and LCP constructs. The Pin-PMMA and LCP constructs were then tested to failure in flexion and left lateral bending.

**Results:** Both the Pin-PMMA and LCP constructs had reduced range of motion at the stabilized L1-L2 vertebral motion unit compared to intact specimens. The Pin-PMMA constructs had less range of motion for the flexion elastic zone than LCP constructs. The Pin-PMMA constructs were stiffer than intact specimens in flexion, extension, and lateral bending, and stiffer than LCP constructs in flexion and left lateral bending. The Pin-PMMA constructs had less angular deformation at construct yield and lower residual deformation at L1-L2 than LCP constructs after destructive testing to failure in flexion. The Pin-PMMA constructs were stiffer, stronger, and had less deformation at yield than LCP constructs after destructive testing to failure in lateral bending. Most construct failed distant to the implant and fixation site.

**Conclusions:** Pin-PMMA constructs had greater lumbar vertebral stiffness and reduced ROM than LCP constructs however, both Pin-PMMA and LCP constructs were stronger than intact specimens.

Pins (or screws) and polymethylmethacrylate (Pin-PMMA) fixation remains a standard of care for vertebral body stabilization of the canine thoracolumbar spine.<sup>1,3-7</sup> Pin-PMMA implants are adaptable to all regions of the vertebral column in any sized dog and provides rigid stabilization.<sup>3,5,6</sup> Unilateral Pin-PMMA constructs are described<sup>5</sup> but most investigations report on bilateral constructs requiring bilateral approaches to the vertebral column.<sup>3-7</sup> Disadvantages of the bilateral approach include prolonged surgery duration and more disruption of the soft tissue and segmental blood supply.<sup>1,2,8</sup> In addition, implantation of PMMA has been associated with persistent infection,<sup>9,10</sup> tissue necrosis leading to compromised periosteal blood supply and superficial bone viability,<sup>11</sup> as well as challenging surgical wound closure.<sup>3,6,12</sup>

The use of a low profile, unilateral locking compression plate (LCP) would address most of the disadvantages of standard, bilateral Pin-PMMA constructs.<sup>13</sup> The LCP can be used bilaterally but only unilateral placement would confer an advantage over Pin-PMMA fixation with a unilateral approach and reduced implant costs. The fixed angle of the locking screw in the plate can make optimum screw placement difficult but use of the LCP eliminates the need for precise contouring of the plate to irregular vertebral surface and allows monocortical screw placement which is less challenging.<sup>14-16</sup>

While bilateral Pin-PMMA or unilateral LCP offer fixation options to the surgeon, no information of their biomechanical performance in the lumbar vertebrae is available. The purpose of this study was to compare the stiffness, angular deformation and mode of failure of bilateral Pin-PMMA constructs to unilateral LCP constructs in an ex vivo model. The hypothesis was that Pin-PMMA lumbar vertebral constructs would be significantly stiffer and have less deformation than LCP constructs.

## MATERIAL AND METHODS

### *Study Design*

Thoracolumbar (T13-L3) vertebral column specimens collected from 16 canine cadavers were assigned equally to one fixation (Pin-PMMA or LCP, n=8 each), matched on the body weight of the cadaver. All specimens were tested before (intact) and after fixation of the L1-L2 vertebral bodies. Outcomes for the T13-L1, L1-L2, and L2-L3 vertebral motion units (VMUs) were compared between the intact specimens and Pin-PMMA and LCP constructs, and between the Pin-PMMA and LCP constructs. Implant placement (pins or screws) within the vertebral bodies was assessed using radiography and computed tomography.

### *Specimen Collection and Preparation*

Thoracolumbar vertebral specimens (T13-L3) were collected from mature canine cadavers (20-35 kg body weight). The dogs had no history of vertebral column disease. Skeletal maturity and the absence of vertebral pathology were confirmed using laterolateral and dorsoventral radiographs (Mark III digital radiography system, Sound-Eklin, Carlsbad, CA). Hypaxial and epaxial musculature, vertebral ligaments (supraspinous and interspinous ligaments, and ligamentum flavum) and joint capsules were preserved. Tissues were kept moist with 0.9% saline solution during preparation, storage, and testing. Specimens were individually wrapped in saline-soaked towels and plastic bags, and stored at -20°C.

Specimens were thawed to room temperature on the day of testing and then mounted in a custom 4-point bending jig (Fig 1). The T13 and L3 vertebrae were secured in fixture pots by inserting Steinman pins (3/32" diameter) transversely through T13 and L3 and embedding the pins and the cranial third of T13 and caudal third of L3 in PMMA (Coe Tray Plastic, GC

America Inc, Alsip, IL). Intact specimens allowed motion at 3 VMUs: T13-L1, L1-L2, and L2-L3.

### *Specimen Testing*

Bending moments were applied to the T13-L3 vertebral segment using a servohydraulic materials testing system (MTS Systems Corp. Eden Prairie, MN) equipped with a 2000 N capacity load cell (Model no. 662.20C-01 MTS Systems Corp). Vertebral body 3-dimensional (3-D) motions were captured using spherical 10 mm diameter retro-reflective markers attached to 1/8" diameter Steinman partially threaded negative profile pins (Imex Veterinary Inc, Longview, Texas) inserted into the dorsal spinous processes.<sup>17</sup> Marker positions (0.05 mm displacement resolution) were tracked at 60 Hz during all tests using video (Fastcam PCI, Photron USA Inc., San Diego, CA).

Nondestructive left and right lateral bending and flexion-extension tests were performed on specimens before and after application of the implants. The order of the test was systematically assigned across specimens to include all possible combinations of test order (Fig 2). Preconditioning was performed under displacement control to a load limit from 1 to -1 Nm bending moment (flexion to extension, left to right lateral bending) at a rate of 0.1 Hz for 5 sinusoidal cycles before each test. Specimens were then loaded for 5 sinusoidal cycles under displacement control to a load limit from 4 Nm to -4 Nm bending moment at 0.1Hz. The 4 Nm load limit was selected as a result of preliminary failure tests of intact and stabilized specimens. The 40 Nm load that was within 60% of the yield load and thus within the elastic region of the specimens. Cyclic tests were run in displacement control because variation in specimen

compliance precluded the ability to run in load control due to mechanical test system tuning limitations.

Destructive testing to failure was then performed on Pin PMMA and LCP specimens using a single ramp load at 10 mm/s in either left lateral bending (4 Pin-PMMA, 4 LCP) or in flexion (4 Pin-PMMA, 4 LCP). The end point was a decrease of bending moment with increasing displacement or to the limit that the constructs allowed, whichever was reached first.

### *Constructs*

**Pin-PMMA.** Two 1/8" or 5/32" (3.2 mm or 4.0 mm) positive profile stainless steel cortical pins (Imex Veterinary Inc, Longview, Texas) were placed in both the L1 and L2 vertebral bodies (Fig 3A-C). On the L1 vertebra, the pins were inserted bilaterally from the dorsolaterocaudal aspect, starting mid-vertebral body at the level of the accessory process, and driven to the ventromediocranial aspect of the vertebra, ending in the cranial aspect of the vertebral body or endplate close to ventral midline. On the L2 vertebra, the pins were inserted bilaterally from the dorsolaterocranial aspect, starting mid-vertebral body at the level of the accessory process and driven ventromedio-caudal to end in the caudal aspect of the vertebral body or endplate close to ventral midline. Pin holes were pre-drilled using a 2.5 mm drill bit and pins were inserted to a depth that ensured threads fully engaged the trans cortex of the vertebral body. Pins were then cut to a length level with the articular facets. Radiographs (laterolateral, dorsoventral) were taken after pin placement to ensure that pins were not compromising the T13-L1 or L2-L3 disc spaces and that each pin appeared to engage cis and trans cortices. Twenty grams of PMMA (Surgical Simplex P, Stryker Haowmedica Osteonics, Mahwah, NJ) were prepared, divided in

half, and applied as a bar around the pins bilaterally at L1-L2 from the bone-pin interface and incorporating the length of the pins.

**LCP.** A 4 hole non-contoured 3.5 mm LCP (DePuy Synthes®, West Chester, PA) was applied to the left lateral aspect of the L1-L2 vertebral bodies (Fig 3D-F) using 4 3.5mm locking screws placed into the locking portion of all Combi-holes. Two 22-gauge hypodermic needles were inserted from dorsolateral into the intervertebral disc to mark the cranial and caudal extent of the L1-L2 disc space. The plate was centered, with the tapered end cranial, over the intervertebral disc space and immediately ventral to the intervertebral foramen. It was held temporarily in place with a push-pull reduction device (DePuy Synthes® 324.024) in the caudal stacked hole. Screws were placed into the 2 plate holes adjacent to the disc, followed by the cranial most plate hole in L1, and the caudal most screw hole (stacked hole) in L2 after removing the push-pull reduction device. Screws were monocortical, to a depth  $\geq 50\%$  of the vertebral body and tightened to 1.5 Nm of torque (DePuy Synthes® torque limiting attachment). Radiographs (laterolateral, dorsoventral) were taken after plate fixation to ensure plate placement over the L1-L2 disc space, and screw placement into the L1-L2 vertebral bodies.

#### *Mechanical Testing Data Reduction*

**Non-destructive analysis.** Data from the 5 consecutive cycles of loading during a test were examined to verify that specimen stiffness and peak loads remained constant during the test. Data from the 3rd cycle were analyzed to avoid potential artifacts from the first and last cycles of each test and the 3rd cycle appeared representative of the 2nd through 4th cycles. Angular deformations of the video markers in each VMU were determined using digitization and processing software (Motus 9, Vicon, Centennial, CO). Marker angular deformations were

transformed to VMU angular deformations by correcting for marker-to-vertebral angle difference using radiographs. For the lateral view of the markers (used during flexion-extension bending) the line representing the vertebral body was drawn along the ventral floor of the canal. For the dorsoventral view of the markers (used during left-right bending), a line was drawn parallel to the sagittal plane separating the vertebral body into equal halves.

Bending moments were determined from the axial loads and geometry of the 4-point bending fixture using the equation  $M = (P/2) \times W$ ; where  $M$  is the bending moment (Nm),  $P$  is the applied load (N), and  $W$  is the distance (m) between the inner and outer swing supports. Bending moment versus angular deformation curves were constructed from the resulting data.

The neutral zone is the region of the bending moment versus angular deformation curve where there is large range of motion with little or no bending moment change<sup>18</sup> (Fig 4). The elastic zone is the region where further angular deformation results in a rise in bending moment in a largely linear, non-damaging manner. In this study, the range of the neutral zone was defined using a standardized procedure for each VMU and each individual specimen. A line of constant bending moment was drawn which separates the flexion and extension portions, or for lateral bending, the left-lateral and right-lateral portions of the curve, into equal parts because they were not always centered about the zero bending moment or zero angular deformation (dashed line, Fig 4). The intersections of the line with the loading curves defined the starts of the neutral zone (points A and B, Fig 4). Each end of the neutral zone was defined by the point on the curve that had a bending moment extending 0.6 Nm beyond the starting bending moment(s). The absolute values of the range are reported, with the sign of the extent designating the direction of loading (positive, flexion or left lateral bending; negative, extension or right lateral bending). The neutral zone stiffness was calculated as the slope of the least-squares linear fit to

the data in the neutral zone. The range of the elastic zone spanned from the end of the neutral zone to 3.5 Nm bending moment. Elastic zone stiffness was determined as the slope of the least-squares linear fit of the data between 2.0 and 3.5 Nm because this region of the curve was linear for all VMUs of all specimens. Energies were calculated as the areas under the respective portions of the curve.

**Failure analysis.** Load versus actuator displacement curves were constructed from single load-to-failure data for the purpose of representing the mechanical properties of whole constructs. The end of the toe-region of the curve and construct yield were determined by detecting respective deviations from curve linearity using sliding least squares regression and 0.08 mm displacement offset criteria. Load and actuator displacement values were converted to bending moment and angular deformation values using construct and load geometries. Construct yield bending moment was the bending moment at the yield point. Construct yield energy was the area under the load-displacement curve from the start of the test to the yield point. Construct stiffness was calculated as the slope of the middle third of the data between the toe of the loading curve and the yield point. Yield angular deformation for each VMU was determined from marker data and construct yield. Residual angular deformation of each VMU was calculated as VMU angle at zero bending moment after specimen unloading. Ultimate strength is not reported since some specimens did not fail (i.e. did not show a decrease in bending moment) within the range of motion constraints within the mechanical test loading.

#### *Failure Mode*

The mode of failure was characterized by observations of radiographs and CT images obtained after destructive failure. Failures were categorized as vertebral fracture versus luxation at the

disc or articulations, and further categorized by site of fracture (T13, L1, L2, L3) or luxation (T12-L1, L1-L2, L2-L3).

### *Statistical Analysis*

**Non-Destructive Tests.** Normality of the outcomes was confirmed by assessing the distribution of the residuals using the Shapiro-Wilks test. Mixed model analysis of variance (ANOVA) that accounted for the repeated measures within a specimen was used to determine the fixed effect of construct (intact, Pin-PMMA, LCP) on the outcomes of ranges of motion, construct stiffness, and energies for flexion-extension and for lateral bending non-destructive tests. Dog was included as a random effect. Analyses were adjusted for the fixed effect of test order (flexion-extension then left-right lateral bending, left-right lateral bending then flexion-extension) to account for any confounding. Post hoc pair-wise comparisons were used to determine differences between constructs using a Tukey adjustment for Type I error. Differences were considered statistically significant when  $P \leq .05$ .

**Destructive Tests.** An analysis of variance was used to determine the fixed effect of construct (LCP, Pin-PMMA) on stiffness and yield bending moment and energy, and on VMU yield and residual angular displacements. Separate analyses were performed for flexion and left lateral bending tests. Dog body weight (kg) was included as a covariate for stiffness, and for yield bending moment and energy because these outcomes are expected to be larger for larger dogs whereas changes in angular displacements are not expected to change with dog size. Least square mean ( $\pm$  standard error) estimates adjusted for body weight were used to compare constructs for stiffness, and yield bending moment and energy. The residual values from the

analyses of variance satisfied the assumption of normality using a Shapiro-Wilk test. Differences were considered statistically significant when  $P \leq .05$ .

**Failure Mode.** The distributions of mode of failure (fracture, luxation) and site of failure (site of fracture (T13, L1, L2, L3) or luxation (T12-L1, L1-L2, L2-L3) between bending modes (flexion, left lateral bending) and between LCP and Pin-PMMA constructs were compared using a Fisher's Exact test with  $P < .05$  considered statistically significant. The failure site was collapsed to a binary categories (L1-L2, distant to L1-L2) for analysis, representing the VMU site of fixation versus an adjacent VMU.

SAS (SAS 9.3, SAS Institute, Cary, NC) was used for all analyses.

#### *Implant Assessment*

Vertebral T13-L3 specimens were radiographed in a neutral position using orthogonal projections to assess implant position and damage from mechanical testing after failure. The specimens also were imaged transversely in 4 mm slices with a helical CT scanner (fx/I helical CT scanner General Electric Co., Milwaukee, WI) using a standardized institutional protocol. Using CT and radiography combined, pin position within the vertebrae of Pin-PMMA constructs were categorized by vertebral purchase (number of cortices engaged), vertebral canal effacement (present or absent) defined as part of the circumference of a pin entering the vertebral canal, and vertebral canal penetration (present or absent) defined as the entire pin circumference within the vertebral canal. Penetration of pins into the intervertebral disc (present or absent) was also recorded. The PMMA was evaluated according to number of pins entirely enclosed within the PMMA and the presence of a solid bone-Pin-PMMA interface.

Screw positions on the LCP constructs were similarly evaluated using CT and radiography. Screws within the vertebral body were categorized by vertebral purchase (<50% or >50% of vertebral body width on CT images), vertebral canal effacement (present or absent) or penetration (present or absent), and intervertebral disc penetration (present or absent). In addition, screws were assessed for whether they remained locked properly in the plate hole after failure.

## RESULTS

### *Implant assessment*

The pins in Pin-PMMA constructs engaged cortices bilaterally in all specimens and did not efface or enter the vertebral canal or disc space(s). The PMMA encased all pins adequately on each construct and bone-Pin-PMMA interface was good in each specimen (Fig 3). All locking screws on LCP constructs were monocortical and engaged  $\geq 50\%$  of the width of the vertebral body (based on transverse CT images). No screws effaced or penetrated the vertebral canal or disc spaces. All screws were adequately locked in plate holes following testing to failure (Fig 3).

### *Mechanical Testing*

**Non-Destructive Test.** Significant differences between constructs for ranges of motion and construct stiffness were detected for flexion-extension at the L1-L2 VMU's (Figs 5A and 6A, Table 1). The LCP and Pin-PMMA constructs had smaller elastic zone and neutral zone ranges compared to intact constructs ( $P \leq .009$  all tests). The flexion elastic zone range was smaller for Pin-PMMA than LCP constructs ( $P = .020$ ). The Pin-PMMA constructs were stiffer in flexion within the elastic zone than LCP constructs ( $P < .001$ ) and intact constructs ( $P < .001$ ). The Pin-

PMMA constructs were also stiffer in extension within the elastic zone than intact constructs ( $P=.002$ ). The stiffness of the LCP constructs were not significantly different in flexion and extension than intact constructs ( $P=.126-.551$ ).

Significant differences between constructs for range of motion and construct stiffness were detected for left and right lateral bending at the L1-L2 VMU (Figs 5B and 6B, Table 2). For left and right lateral bending, LCP and Pin-PMMA constructs had smaller elastic zone and neutral zone ranges compared to intact constructs ( $P<.001$  all tests). For left and right lateral bending, Pin-PMMA but not LCP constructs were stiffer within the elastic zone than intact constructs ( $P=.035$ ,  $P <.001$ , respectively). For left lateral bending, Pin-PMMA constructs were stiffer within the elastic zone than LCP constructs ( $P=.002$ ). LCP constructs were stiffer in the elastic zone in right lateral bending than in left lateral bending ( $P=.027$ ).

There were no significant differences between constructs for range of motion or stiffness for the T13-L1 VMU. At the L2-L3 VMU, Pin-PMMA constructs had a significantly smaller extension elastic zone range ( $P=.002$ ) and greater elastic zone stiffness ( $P=.011$ ) than intact constructs. In right-lateral bending, LCP constructs had greater stiffness than intact constructs at the L2-L3 VMU ( $P=.035$ ).

**Failure Tests.** For all constructs combined, stiffness was significantly higher in flexion than in lateral bending ( $P=.005$ ), and L1-L2 had lower residual angular deformation in flexion than lateral bending ( $P=.021$ ). For failure in flexion, Pin-PMMA constructs had significantly lower L1-L2 angular deformation at construct yield and residual angle (deformation) after the test than LCP construct's (Table 3). For failure in left-lateral bending, Pin-PMMA constructs had greater

stiffness, greater yield strength, and lower L1-L2 yield residual deformation than LCP constructs (Table 4).

**Failure Mode.** The distributions of mode of failure (fracture, luxation) was not significantly different between Pin-PMMA and LCP constructs ( $P=1.0$ ) or between failure test type ( $P=.119$ ). Most (6/9) lateral bending tests failed by bone fracture whereas most (5/7) flexion tests failed by luxation. Most failures occurred outside of the L1-L2 VMU (i.e., T13, L3 or T13-L1, L2-L3 disc or articulations) and site did not differ between Pin-PMMA and LCP constructs ( $P=.323$ ). Three Pin-PMMA constructs and 1 LCP construct failed in at the L1-L2 VMU. All failures that involved the L1-L2 VMU were lateral bending tests (4/9) but none of the 7 flexion tests ( $P=.088$ ).

## DISCUSSION

This study shows that Pin-PMMA and LCP constructs significantly reduce the range of motion in non-destructive bending tests over that of the intact spine however, there were some important differences between the two constructs. Pin-PMMA constructs had significantly lower range of motion and greater stiffness in flexion than LCP constructs. In vertebral fractures or luxations, the canine spine has been shown to lose its ability to withstand forces in flexion when the ventral components of the vertebral column are fractured.<sup>19</sup> Since the predominant motion in the thoracolumbar vertebral column in dogs is flexion and extension, these motions are the most important to counteract at this location.<sup>3,19</sup> Based on an understanding of these forces, bilateral Pin-PMMA constructs may be indicated over unilateral LCP in cases of vertebral body fracture, circumferential disc breakdown or conditions where both dorsal and ventral stabilizing structures are affected bilaterally.<sup>19-24</sup>

In contrast, LCP fixation may be indicated, and even optimal, in animals where increasing the stability of the vertebral column is important such as disease states where excessive motion is part of the underlying pathogenesis. Abnormal vertebral column mobility in these situations is often not overtly unstable and may preferentially affect one side.<sup>3</sup> Application of a unilateral LCP if one side is preferentially affected may allow greater than normal range of movement between 2 vertebrae, especially in lateral spinal bending. Dogs with congenital bony malformation from hypoplastic facet formation or secondary to hemi-laminectomy (where stabilizing elements have been surgically removed) may benefit from unilateral LCP fixation and thus also avoid the disadvantages of Pin-PMMA constructs. It is possible that unilateral LCP stabilization may be sufficient for selected, anatomically reduced, non-complicated vertebral stabilizations, consistent with successful unilateral DCP vertebral stabilizations in dogs.<sup>25</sup>

Right and left lateral bending tests showed the stiffness of the Pin-PMMA constructs was not different in right and left lateral bending. As expected, the stiffness of LCP constructs differed significantly from one side to the other. Since the LCP was placed on the left lateral aspect of the tested VMUs, in right lateral bending, the LCP functions as a tension band on the left side and effectively reduces lateral bending in that direction. Conversely, in left lateral bending, there is no tension band effect on the right side allowing for greater range of motion. Stiffness of the LCP construct was not different to that of the Pin-PMMA construct in right lateral bending. Thus, application of a unilateral LCP should be on the side where reduced laterolateral movement is required. In the case of vertebral fracture luxation with concurrent unilateral fracture of a facet articulation, the LCP should be applied on the same (ipsilateral) side as the facet disruption.

Destructive testing resulted in failure of outside of the L1-L2 fixation, regardless of the construct. Thus, both constructs likely provide greater stability at treated joints than the inherent stability at adjacent unaffected joints and may facilitate healing of anatomically reduced instability. Since these tests were done on an intact spinal segment, it is unknown if they provide sufficient stability for healing of complex vertebral fractures. However, vertebral fractures repaired with a very rigid fixation and anatomic reconstruction (gap <1mm) should have direct bone healing,<sup>1,5</sup> which is optimal in the canine spine to avoid callus formation and potential compression of local neurological structures.

Bending tests of constructs have inherent limitations since the model obviates the in vivo influences of surrounding musculature, fascial planes, and abdominal muscles that can prevent abnormal motion or load on the vertebrae during movement of vertebral motion units. However, with neurologic dysfunction, these elements may provide insufficient protection. Specimens in the current study were only tested in flexion-extension and lateral bending. Flexion and extension (ventral-dorsal bending) are considered primary motions of the spine where the motion only occurs in the direction of the applied force, however 3-D motion patterns of the thoracolumbar spine have not been defined in dogs.

Torsional properties were not investigated in the current study. Coupling of motion in the cervical spine is well documented in people and has also been reported in dogs.<sup>17,26</sup> That is, lateral bending is accompanied by axial rotation. In the current study, motion coupling was constrained. It has been shown in an ex vivo canine tibial gap model that monocortical screws in LCP constructs have lower stiffness than bicortical screw LCP plated constructs.<sup>15</sup> However, in the forearm, unicortical locking screws that were 75% inserted into the bone were equivalent to bicortical screws.<sup>27,28</sup> Thus, the LCP plate construct in the current study may have performed

better with bicortical or monocortical far-cortex abutting screws.<sup>29</sup> Unicortical and bicortical locking screw constructs have not been comparatively tested in the lumbar spine however, bicortical screw constructs may be more beneficial for counteracting torsional loads.<sup>30</sup>

The extent of flexion-extension of this ex vivo model was restricted due to the limits of machine fixture space which prevented the spines from reaching maximum failure. However, at a minimum, all spines were bent to yield (permanent) deformation that would represent vertebral column failure in the live animal. The conversion of linear actuator displacement to angular motion is a potential drawback of the testing since the angular deformation rate is faster as the angle increases, and thus, faster nearer the extremes of linear actuator displacement. The effects of different angular deformation rates among treatment conditions and within tests are unknown but because the load rate was relatively slow for all tests and the effects of different treatments are large, it is assumed that effects of load rate on the results are relatively small and negligible.

This study found that bilateral Pin-PMMA constructs were stiffer than unilateral LCP constructs in flexion, extension and lateral bending at the L1-2 VMU in intact spines. However, the LCP was as stiff as the intact spines and decreased range of motion compared to the intact spine. The differences elucidated by these in vitro findings may help guide clinicians in choosing the most appropriate method of fixation based on underlying vertebral column pathology and the degree of stabilization required.

## ACKNOWLEDGEMENTS

Funding was provided by AO Foundation Grant AOVET-12-02K and the Center for Companion Animal Health, University of California-Davis Grant 2012-29-F. Implants were donated by DePuy SynthesVet and Imex.

## DISCLOSURE

The authors declare no conflicts of interest related to this report.

## REFERENCES

1. Tobias KM, Johnston SA: *Veterinary surgery: Small animal*. St. Louis, Mo., Elsevier, 2012
2. Sharp NJH, Wheeler SJ: *Small animal spinal disorders: Diagnosis and surgery* (edn 2). Philadelphia, PA, Elsevier Mosby, 2005
3. Jeffery ND: Vertebral fracture and luxation in small animals. *Vet Clin North Am Small Anim Pract* 2010;40:809-828
4. Bruecker KA, Seim HB: Principles of spinal fracture management. *Semin Vet Med Surg* 1992;7:71-84
5. Johnson AL, Houlton JEF, Vannini R: *AO Principles of fracture management in the dog and cat*. New York, NY, Thieme, 2005
6. Blass C, Seim H: Spinal fixation in dogs using Steinman pins and methylmethacrylate. *Vet Surg* 1984;13:203-210
7. Aikawa T, Kanazono S, Yoshigae Y, et al: Vertebral stabilization using positively threaded profile pins and polymethylmethacrylate, with or without laminectomy, for spinal canal stenosis and vertebral instability caused by congenital thoracic vertebral anomalies. *Vet Surg* 2007;36:432-441
8. Parker AJ: Clinical significance of traumatic occlusion of segmental spinal arteries. *J Am Vet Med Assoc* 1973;162:1041-1042
9. Turk R, Singh A, Weese JS: Prospective surgical site infection surveillance in dogs. *Vet Surg* 2015;44:2-8

0. van de Belt H, Neut D, Schenk W, et al: Infection of orthopedic implants and the use of antibiotic-loaded bone cements. A review. *Acta Orthop Scand* 2001;72:557-571
1. Roush JK, Wilson JW: Effects of plate luting on cortical vascularity and development of cortical porosity in canine femurs. *Vet Surg* 1990;19:208-214
2. Sturges BK, LeCouteur RA: Vertebral Fractures and Luxations, in Slatter DH (ed): *Textbook of small animal surgery* (ed 3rd), Vol. Philadelphia, W.B. Saunders, 2002.
3. Miller DL, Goswami T: A review of locking compression plate biomechanics and their advantages as internal fixators in fracture healing. *Clin Biomech (Bristol, Avon)* 2007;22:1049-1062
4. Egol KA, Kubiak EN, Fulkerson E, et al: Biomechanics of locked plates and screws. *J Orthop Trauma* 2004;18:488-493
5. Demner D, Garcia TC, Serdy MG, et al: Biomechanical comparison of mono- and bicortical screws in an experimentally induced gap fracture. *Vet Comp Orthop Traumatol* 2014;27:422-429
6. Goh CS, Santoni BG, Puttlitz CM, et al: Comparison of the mechanical behaviors of semicontoured, locking plate-rod fixation and anatomically contoured, conventional plate-rod fixation applied to experimentally induced gap fractures in canine femora. *Am J Vet Res* 2009;70:23-29
7. Agnello KA, Kapatkin AS, Garcia TC, et al: Intervertebral biomechanics of locking compression plate monocortical fixation of the canine cervical spine. *Vet Surg* 2010;39:991-1000
8. Wilke HJ, Wenger K, Claes L: Testing criteria for spinal implants: recommendations for the standardization of in vitro stability testing of spinal implants. *Eur Spine J* 1998;7:148-154

9. Smith GK, Walter MC: Spinal decompressive procedures and dorsal compartment injuries: comparative biomechanical study in canine cadavers. *Am J Vet Res* 1998;49:266-273
10. Shires PK, Waldron DR, Hedlund CS: A biomechanical study of rotational instability in unaltered and surgically altered canine thoracolumbar vertebral motion units. *Prog Vet Neur* 1991;2:6-14
11. Hill TP, Lubbe AM, Guthrie AJ: Lumbar spine stability following hemilaminectomy, pediculectomy, and fenestration. *Vet Comp Orthop Traumatol* 2000;13:165-171
12. Revés NV, Bürki A, Ferguson S, et al: Influence of partial lateral corpectomy with and without hemilaminectomy on canine thoracolumbar stability: A biomechanical study. *Vet Surg* 2012;41:228-234
13. Arthurs G: Spinal instability resulting from bilateral mini-hemilaminectomy and pediculectomy. *Vet Comp Orthop Traumatol* 2009;22:422-426
14. Schulz KS, Waldron DR, Grant JW, et al: Biomechanics of the thoracolumbar vertebral column of dogs during lateral bending. *Am J Vet Res* 1996;57:1228-1232
15. Swaim SF: *Vertebral Body Plating for Spinal Immobilization*. *J Am Vet Med Assoc* 1971;158:1683-1695
16. Hofstetter M, Gedet P, Doherr M, et al: Biomechanical analysis of the three-dimensional motion pattern of the canine cervical spine segment C4-C5. *Vet Surg* 2009;38:49-58
17. Liu X, Wu W, Fang Y, Zhang M, et al: Biomechanical comparison of osteoporotic distal radius fractures fixed by distal locking screws with different length. *Plos One* 2014;9:1-9

8. Wall L, Brodt M, Silva M, et al: The effects of screw length on stability of simulated osteoporotic distal radius fractures fixed with volar locking plates. *J Hand Surg Am* 2012;37A:446-453
9. Overturf S, Morris R, Gugala Z, et al: Biomechanical comparison of bicortical locking versus unicortical far-cortex--abutting locking screw-plate fixation for comminuted radial shaft fractures. *J Hand Surg Am* 2014;39:1907-1913
10. Pater T, Grindel S, Schmeling G, et al. Stability of unicortical locked fixation versus bicortical non-locked fixation for forearm fractures. *Bone Research* 2014;2:1-5

Accepted Article

Figure 1 Materials testing system, with a T13-L3 vertebral column segment, in the custom 4-point bending jig. Reflective markers were attached to bars inserted into the spinous processes of L1 and L2 vertebrae to track motion of these vertebrae with 2 more reflective markers attached to each fixture pot to track movement of the T13 and L3 vertebral bodies.

Figure 2 Study design for non-destructive and failure tests for intact and LCP or Pin-PMMA constructs. Note for 8 LCP stabilized constructs, 3 constructs were tested in flexion and 5 constructs were tested in left lateral bending.

Figure 3 (A) Left lateral view of Pin-PMMA construct. (B) Dorsoventral radiograph. (C) Transverse computed tomography image. (D) Left lateral view of LCP construct. (E) Dorsoventral radiograph. (E) Transverse computed tomography.

Figure 4 Bending moment versus angular deformation curve. The loading portion is the thick grey line, the unloading portion is the thin black line. The separation between flexion-extension or left-right lateral bending is the dotted black line (point A to point B). NZ neutral zone, EZ elastic zone, EZS elastic zone stiffness (black dashed line).

Figure 5. Non-destructive range of motion (ROM) of vertebral motion units (VMU). (A) Flexion-extension. (B) Right and left lateral bending. Each shaded bar is the mean range of either flexion (Flex) or extension (Ext), or right or left lateral bending, within the neutral zone (NZ) or the elastic zone (EZ).

Figure 6. Stiffness of vertebral motion units. (A) Flexion-extension. (B) Right and left lateral bending. Each shaded bar is the mean range of either flexion (Flex) or extension (Ext), or right or left lateral bending, within the neutral zone (NZ) or the elastic zone (EZ).

Accepted Article

**Table 1** Mean (95% confidence interval) neutral zone (NZ) and elastic zone (EZ) range and stiffness for flexion-extension non-destructive testing for T13-L1, L1-L2, and L2-L3 vertebral motion units. Within a row, means with the same superscript are not significantly different.

	Intact	LCP	Pin-PMMA
<b>T13-L1 Flexion</b>			
NZ range (°)	5.0 <sup>a</sup> (4.1 - 5.9)	5.0 <sup>a</sup> (3.4 - 6.6)	4.1 <sup>a</sup> (3.0 - 5.1)
NZ stiffness (Nm/°)	-0.13 <sup>a</sup> (-.16 - -0.10)	-0.13 <sup>a</sup> (-.17 - -.09)	-0.16 <sup>a</sup> (-.22 - -.10)
EZ range (°)	6.3 <sup>a</sup> (5.5 - 7.1)	5.5 <sup>a</sup> (4.4 - 6.5)	6.7 (5.5 - 7.9)
EZ stiffness (Nm/°)	-0.96 <sup>a</sup> (-1.11 - -0.82)	-1.11 <sup>a</sup> (-1.38 - -0.84)	-0.86 <sup>a</sup> (-1.04 - -0.69)
<b>T13-L1 Extension</b>			
NZ range (°)	-5.4 <sup>a</sup> (-6.7 - -4.1)	-4.7 <sup>a</sup> (-6.0 - -3.4)	-4.1 <sup>a</sup> (-4.8 - -3.3)
NZ stiffness (Nm/°)	-0.13 <sup>a</sup> (-0.17 - -0.09)	-0.12 <sup>a</sup> (-0.18 - -0.06)	-0.13 <sup>a</sup> (-0.17 - -0.09)
EZ range (°)	-5.0 <sup>a</sup> (-5.5 - -4.4)	-4.9 <sup>a</sup> (-5.6 - -4.3)	-4.5 <sup>a</sup> (-5.3 - -3.8)
EZ stiffness (Nm/°)	-1.12 <sup>a</sup> (-1.29 - -0.94)	-1.08 <sup>a</sup> (-1.37 - -0.80)	-1.27 <sup>a</sup> (-1.63 - -0.92)
<b>L1-L2 Flexion</b>			
NZ range (°)	3.0 <sup>a</sup> (2.5 - 3.5)	0.2 <sup>b</sup> (-0.1 - 0.6)	0.0 <sup>b</sup> (0.0 - 0.1)
NZ stiffness (Nm/°)	-0.20 <sup>a</sup> (-0.26 - -0.17)	-2.83 <sup>a</sup> (-12.24 - 6.58)	-1.11 <sup>a</sup> (-10.03 - 7.80)

EZ range (°)	4.0 <sup>a</sup> (3.3 - 4.7)	1.7 <sup>b</sup> (0.9 - 2.5)	0.5 <sup>c</sup> (0.3 - 0.6 - 0)
EZ stiffness (Nm/°)	-1.98 <sup>a</sup> (-2.41 - -1.56)	-1.91 <sup>a</sup> (-2.40 - -1.42)	-6.06 <sup>b</sup> (-8.15 - -3.97)
<b>L1-L2 Extension</b>			
NZ range (°)	-3.1 <sup>a</sup> (-3.8 - -2.4)	-0.2 <sup>b</sup> (-0.5 - 0.0)	-0.1 <sup>b</sup> (-0.2 - 0.0)
NZ stiffness (Nm/°)	-0.20 <sup>a</sup> (-0.25 - -0.15)	-1.86 <sup>a</sup> (-6.24 - 2.51)	0.88 <sup>a</sup> (-10.96 - 12.72)
EZ range (°)	-3.3 <sup>a</sup> (-3.6 - -3.1)	-1.4 <sup>b</sup> (1.9 - -0.9)	-0.7 <sup>b</sup> (-0.9 - -0.5)
EZ stiffness (Nm/°)	-1.51 <sup>a</sup> (-1.72 - -1.31)	-2.89 <sup>ab</sup> (-4.59 - -1.19)	-4.61 <sup>b</sup> (-6.30 - -2.91)
<b>L2-L3 Flexion</b>			
NZ range (°)	3.6 <sup>a</sup> (2.9 - 4.3)	3.9 <sup>a</sup> (2.8 - 4.9)	2.9 <sup>a</sup> (2.4 - 3.3)
NZ stiffness (Nm/°)	-0.18 <sup>a</sup> (-0.21 - -0.14)	-0.16 <sup>a</sup> (-0.20 - -0.12)	-0.21 <sup>a</sup> (-0.25 - -0.17)
EZ range (°)	4.7 <sup>a</sup> (4.1 - 5.4)	4.2 <sup>a</sup> (3.1 - 5.3)	5.0 <sup>a</sup> (4.0 - 6.1)
EZ stiffness (Nm/°)	-1.30 <sup>a</sup> (-1.52 - -1.10)	-1.48 <sup>a</sup> (-1.95 - -1.00)	-1.20 <sup>a</sup> (-1.49 - -0.92)
<b>L2-L3 Extension</b>			
NZ range (°)	-3.7 <sup>a</sup> (-4.2 - -3.1)	-3.7 <sup>a</sup> (-4.6 - -2.8)	-3.1 <sup>a</sup> (-3.5 - -2.6)
NZ stiffness (Nm/°)	-0.16 <sup>a</sup> (-0.20 - -0.12)	-0.15 <sup>a</sup> (-0.23 - -0.07)	-0.18 <sup>a</sup> (-0.24 - -0.12)
EZ range (°)	-3.9 <sup>a</sup> (4.1 - 5.4)	-3.6 <sup>ab</sup> (3.1 - 5.3)	-3.2 <sup>b</sup> (4.0 - 6.1)
EZ stiffness (Nm/°)	-1.37 <sup>a</sup>	-1.44 <sup>ab</sup>	-2.0 <sup>b</sup>

(-1.52 - -1.10) (-1.95 - -1.00) (-1.49 - -0.92)

---

Accepted Article

Table 2 Mean (95% confidence interval) neutral zone (NZ) and elastic zone (EZ) range and stiffness for left-right lateral bending non-destructive for T13-L1, L1-L2, and L2-L3 vertebral motion units. Within a row, means with the same superscript are not significantly different.

	Intact	LCP	Pin-PMMA
<b>T13-L1 Left</b>			
NZ range (°)	5.5 <sup>a</sup> (4.5 - 6.5)	6.0 <sup>a</sup> (4.4 - 7.7)	5.4 (4.4 - 6.4)
NZ stiffness (Nm/°)	-0.11 <sup>a</sup> (-0.14 - -0.09)	-0.1 <sup>a</sup> (-0.13 - -0.07)	-0.11 <sup>a</sup> (-0.14 - -0.08)
EZ range (°)	5.6 <sup>a</sup> (5.0 - 6.3)	5.6 <sup>a</sup> (4.0 - 7.2)	6.4 <sup>a</sup> (5.2 - 7.6)
EZ stiffness (Nm/°)	-0.85 <sup>a</sup> (-0.96 - -0.74)	-0.95 <sup>a</sup> (-1.22 - -0.67)	-0.79 <sup>a</sup> (-0.91 - -0.66)
<b>T13-L1 Right</b>			
NZ range (°)	-6.1 <sup>a</sup> (-7.0 - -5.2)	-6.4 <sup>a</sup> (-7.7 - -5.1)	-5.9 <sup>a</sup> (-7.2 - -4.7)
NZ stiffness (Nm/°)	-0.11 <sup>a</sup> (-0.15 - -0.07)	-0.08 <sup>a</sup> (-0.11 - -0.04)	-0.12 <sup>a</sup> (-0.17 - -0.06)
EZ range (°)	-5.7 <sup>a</sup> (-6.4 - -5.0)	-5.4 <sup>a</sup> (-6.1 - -4.7)	-5.7 <sup>a</sup> (6.6 - -4.9)
EZ stiffness (Nm/°)	-0.86 <sup>a</sup> (-0.95 - -0.76)	-0.86 <sup>a</sup> (-0.98 - -0.75)	-0.85 <sup>a</sup> (-1.02 - -0.68)
<b>L1-L2 Left</b>			
NZ range (°)	7.0 <sup>a</sup> (5.9 - 8.0)	0.3 <sup>b</sup> (0.1 - 0.4)	0.1 <sup>b</sup> (-0.1 - 0.3)

NZ stiffness (Nm/°)	-0.08 <sup>a</sup> (-0.09 - -0.07)	-1.24 <sup>a</sup> (-5.19 - 2.71)	-1.1 <sup>a</sup> (-8.90 - 6.70)	-
EZ range (°)	5.8 <sup>a</sup> (4.9 - 6.7)	1.0 <sup>b</sup> (0.4 - 1.5)	0.3 <sup>b</sup> (0.1 - 0.6)	
EZ stiffness (Nm/°)	-0.92 <sup>a</sup> (-1.02 - -0.83)	-3.86 <sup>a</sup> (-5.07 - 2.66)	-12.91 <sup>b</sup> (-18.00 - 7.81)	-
<b>L1-L2 Right</b>				
NZ range (°)	-7.6 <sup>a</sup> (-8.5 - -6.7)	-0.3 <sup>b</sup> (-0.5 - -0.1)	-0.2 <sup>b</sup> (-0.4 - 0.0)	
NZ stiffness (Nm/°)	-0.09 <sup>a</sup> (-0.13 - -0.06)	-0.66 <sup>a</sup> (-4.45 - 3.13)	-2.25 <sup>a</sup> (-5.92 - 1.42)	-
EZ range (°)	-5.9 <sup>a</sup> (-6.6 - -5.2)	-0.7 <sup>b</sup> (-1.1 - -0.3)	-0.3 <sup>b</sup> (-0.5 - -0.1)	
EZ stiffness (Nm/°)	-0.87 <sup>a</sup> (-0.94 - -0.80)	-6.88 <sup>ab</sup> (-12.74 - 1.01)	-34.12 <sup>b</sup> (-20.81 - 6.27)	-
<b>L2-L3 Left</b>				
NZ range (°)	7.5 <sup>a</sup> (6.2 - 8.8)	7.1 <sup>a</sup> (5.8 - 8.4)	7.3 (5.1 - 9.5)	
NZ stiffness (Nm/°)	-0.08 <sup>a</sup> (-0.09 - -0.07)	-0.08 <sup>a</sup> (-0.10 - -0.06)	-0.08 (-0.10 - 0.06)	-
EZ range (°)	5.9 <sup>a</sup> (5.1 - 6.6)	5.5 <sup>a</sup> (4.1 - 6.9)	6.5 <sup>a</sup> (5.1 - 7.9)	
EZ stiffness (Nm/°)	-0.92 <sup>a</sup> (-1.03 - -0.81)	-1.07 <sup>a</sup> (-1.50 - -0.64)	-0.82 <sup>a</sup> (-0.94 - 0.69)	-

**L2-L3 Right**

NZ range (°)	-7.5 <sup>a</sup> (-8.5 - -6.5)	-7.5 <sup>a</sup> (-8.5 - -6.6)	7.6 <sup>a</sup> (-8.9 - -6.3)
NZ stiffness (Nm/°)	-0.09 <sup>a</sup> (-0.13 - -0.06)	-0.07 <sup>a</sup> (-0.11 - -0.02)	-0.08 <sup>a</sup> (-0.11 - -0.05)
EZ range (°)	-6.3 <sup>a</sup> (-7.2 - -5.3)	-5.4 <sup>a</sup> (-6.9 - -3.9)	-6.3 <sup>a</sup> (-7.4 - -5.1)
EZ stiffness (Nm/°)	-0.82 <sup>a</sup> (-0.92 - -0.71)	-0.98 <sup>b</sup> (-1.21 - -0.74)	-0.84 <sup>ab</sup> (-0.96 - -0.71)

Table 3 - Mean (SD) dog weight and L1-L2 length and mean (95% confidence interval) results of flexion failure testing.

	LCP	n	Pin-PMMA	n
Body weight (kg)	24.8 (3.6)	3	28.9 (3.5)	3
L1-L2 Length (cm)	5.4 (0.5)	3	5.8 (0.3)	4
Stiffness (Nm/°)*	79 (7 - 151)	3	98.1 (72.8 - 123.4)	4
Yield Angular Deformation (°)				
T13-L1	17.8	3	16.9	4

	(5.1 - 30.5)		(15.3 - 18.6)	
L1-L2	7.3 (1.9 - 12.7)	3	3.3 (2.2 - 4.4)	4
L2-L3	20.5 (-6.1 - 47.2)	3	12.9 (8.4 - 17.4)	4
Yield Bending Moment (Nm)*	30.3 (52.5 - 8.0)	3	29.3 (24.1 - 34.4)	4
Yield Energy (Nm*°)*	7740 (1227 - 14253)	3	6415 (4540 - 8290)	4
Residual Angle (°)				
T13-L1	14.9 (-29.1 - 58.9)	3	10.3 (7.5 - 13.0)	4
L1-L2	2.1† (1.6 - 2.6)	3	-0.5 (-2.9 - 1.9)	4
L2-L3	7.1 (-1.6 - 15.9)	3	8.7 (-3.3 - 20.7)	4

\*Means adjusted for body weight.

†LCP means significantly different from Pin-PMMA

**Table 4** Mean (SD) dog weight and L1-L2 length and mean (95% confidence interval) results of left lateral bending failure testing.

	LCP	n	Pin-PMMA	n
Body weight (kg)	24.9 (7.90)	4	19.8 (5.5)	4
L1-L2 Length (cm)	5.4 (0.5)	5	5.8 (0.1)	4
Stiffness (Nm/°)*	51.7† (37.8 - 65.5)	5	69.2 (61.9 - 76.5)	4
Yield Angular Deformation (°)				
T13-L1	19.7 (15.3 - 24.0)	5	21.0 (14.9 - 27.0)	4
L1-L2	5.4† (2.9 - 8.0)	5	2.3 (-0.2 - 4.9)	4
L2-L3	18.0 (14.9 - 21.2)	5	18.0 (13.5 - 22.4)	4
Yield Bending Moment (Nm)*	21.5† (11.2 - 31.7)	5	28.7 (15.6 - 41.8)	4
Yield Energy (Nm*°)*	6612 (2046 - 11179)	5	8663 (2165 - 15161)	4
Residual Angle (°)				
T13-L1	11.0 (7.3 - 14.8)	4	17.3 (7.4 - 27.1)	4
L1-L2	3.1 (0.0 - 6.1)	4	1.9 (1.2 - 2.7)	4
L2-L3	9.5 (-1.1 - 20.1)	4	5.2 (-0.3 - 10.7)	4

\*Means adjusted for body weight.

†LCP means significantly different from Pin-PMMA